Bioorganic & Medicinal Chemistry 20 (2012) 2490–2497

Contents lists available at SciVerse ScienceDirect

Bioorganic & Medicinal Chemistry

journal homepage: www.elsevier.com/locate/bmc

Exogenous fluorescent tracer agents based on pegylated pyrazine dyes for real-time point-of-care measurement of glomerular filtration rate

Amruta R. Poreddy *, William L. Neumann †, John N. Freskos, Raghavan Rajagopalan, Bethel Asmelash, Kimberly R. Gaston, Richard M. Fitch, Karen P. Galen, Jeng-Jong Shieh, Richard B. Dorshow

Covidien Pharmaceuticals, 675 McDonnell Boulevard, Hazelwood, MO 63042, USA

ARTICLE INFO

Article history:
Received 19 January 2012
Revised 1 March 2012
Accepted 5 March 2012
Available online 10 March 2012

Keywords:
Glomerular filtration rate
GFR
Renal function
Renal clearance
Fluorescence
Pyrazine carboxamides
Pegylation

ABSTRACT

Novel pyrazine carboxamides bearing hydrophilic poly(ethylene glycol) (PEG) moieties were designed, synthesized, and evaluated for use as fluorescent glomerular filtration rate (GFR) tracer agents. Among these, compounds **4d** and **5c** that contain about 48 ethylene oxide units in the PEG chain exhibited the most favorable physicochemical and renal clearance properties. In vitro studies show that these two compounds have low plasma protein binding, a necessary condition for renal excretion. In vivo animal model results show that **4d** and **5c** have a higher urine recovery of the injected dose than iothalamate (a commonly considered gold standard GFR agent). Pharmacokinetic studies show that these two compounds exhibit a plasma clearance equivalent to iothalamate, but with a faster (i.e. lower) terminal half-life than iothalamate (possibly from restricted distribution into the extracellular space due to large molecular size and hydrodynamic volume). Furthermore, the plasma clearance of **4d** and **5c** remained unchanged upon blockage of the tubular secretion pathway with probenecid, a necessary condition for establishment of clearance via glomerular filtration exclusively. Finally, noninvasive real-time monitoring of this class of compounds was demonstrated by pharmacokinetic clearance of **5c** by optical measurements in rat model, which correlates strongly with plasma concentration of the tracer. Hence, **4d** and **5c** are promising candidates for translation to the clinic as exogenous fluorescent tracer agents in real-time point-of-care monitoring of GFR.

1. Introduction

Glomerular filtration rate (GFR), which measures the amount of ultrafiltrate of plasma produced by kidney within a given time, is now widely accepted as the best indicator of renal function in the state of health and disease. The clinical guidelines formulated by the National Kidney Foundation advocate use of GFR in the staging of kidney disease brought about by chronic or acute clinical, physiological, and pathological conditions.[1] Driven primarily by the low-cost and convenience, endogenous serum creatinine[2,3] and estimated GFR (eGFR)[4,5] based on serum creatinine concentration continue to be widely reported by clinical laboratories as a first line test of renal function despite the many known limitations of these methods.[6–8] Measured GFR using urinary or plasma clearance of exogenous tracer agents[9] is highly desirable because it will obviate the variability imposed by anthropometric factors. Therefore, for the past decade, the use of non-radioactive iothalamate (sodium 5-acetamido-2,4,6-triiodo-*N*-methylisophthalamate)[10,11] has become the standard of practice for the measurement of GFR. However, complexity of measurement protocols such as the time consuming HPLC analysis of plasma samples makes this method unsuitable for continuous monitoring of renal function at the bedside. Real-time monitoring of renal function was originally demonstrated by Rabito et al.[12,13] by measurement of clearance of the glomerular filtration agent ^{99m}Tc-DTPA, involves undesirable handling and disposal of radioactivity. Thus, there is considerable interest in the development of exogenous fluorescent tracers for the continuous, real-time, and accurate measurement of GFR via transcutaneous fluorescent methods using dye conjugates[14–18] and metal complexes.[19,20] Utilization of FITC-inulin[15,17] and FITC-sinistrin[16,18] involves the complications associated with availability in pure form and immunogenicity of the polysaccharides, whereas metal complexes like carbostyril124-DTPA-Eu involves unfavorable physicochemical properties that is, excitation of the tracer occurring in the UV region.[19]

We had recently successfully demonstrated that hydrophilic small molecule pyrazine carboxamide derivatives of the type **2**

Abbreviations: GFR, glomerular filtration rate; FITC, fluorescein isothiocyanate; DTPA, diethylenetriaminepentaacetate; EDTA, ethylenediaminetetraacetic acid; ECF, extracellular fluid; PEG, polyethylene glycol; MWCO, molecular weight cut-off; PPB, plasma protein binding; %ID, percent injected dose; PBS, phosphate buffered saline.

* Corresponding author. Tel.: +1 314 654 8328; fax: +1 314 654 1573.
E-mail address: amruta.poreddy@covidien.com (A.R. Poreddy).
† Current address: Department of Pharmaceutical Sciences, Southern Illinois University, 220 University Park Drive, Edwardsville, IL 62026, United States.

0968-0896/$ - see front matter © 2012 Elsevier Ltd. All rights reserved.
http://dx.doi.org/10.1016/j.bmc.2012.03.015

and **3** derived from 3,6-diaminopyrazine-2,5-dicarboxylic acid (**1**) are viable exogenous fluorescent tracers for the measurement of GFR (Fig. 1).[21] However, being small molecules (MW <500 Da), these pyrazine derivatives distribute rather freely into the extracellular fluid (ECF), resulting in a volume of distribution (V_d) similar to that of iothalamate, and consequently, leads to longer clearance time than those agents that do not diffuse into the extracellular space. In some applications of this real-time point-of-care GFR determination methodology, there is an advantage to minimizing the time duration needed to accomplish the measurement. For example, prior to administration of X-ray or magnetic resonance contrast media, clinicians require a real-time and rapid renal function assessment such that the usual work flow and throughput in handling patients is maintained. A GFR agent with a larger rate constant than the previous constructs may be ideal for such an application. Since k ≈GFR/V_d, where k is the rate constant (inversely proportional to the time constant or terminal half-life), decreasing the volume of distribution will result in faster clearance.[22] Therefore, our strategy to accomplish just such a construct would be to modify the size of pyrazine derivatives such that it would be substantially restricted to the vasculature, thus reducing diffusion into the tissue.

These considerations led to the investigation of poly(ethylene glycol) (PEG) derivatives of our pyrazine scaffold. PEG groups being biocompatible, non-immunogenic, and non-toxic have been used to modify therapeutic drugs for enhancement of their pharmacokinetic performance in vivo.[23,24] Correlation studies between PEG molecular weight and half-life in blood circulation after intravenous administration in mice have shown that small PEGs are more rapidly cleared than large ones. For example, the half-life increases from 18 min to 1 day as the molecular weight increases from 6 to 190 kDa, and moderate molecular weight PEG chains (<6 kDa) are known to be filtered by the glomerulus and not reabsorbed by the renal tubules.[25] It seems reasonable that pegylated pyrazine constructs which are small enough to be filtered freely by the kidneys, but of significantly larger hydrodynamic volume than small molecules, should be more confined to the vasculature and less freely distributed in the ECF. Thus we hypothesized that these moderate molecular weight (<6 kDa) pegylatged pyrazines would have higher renal clearance rate constants which would translate into a less time-consuming bedside GFR measurement. Accordingly, we wish to report the results of our structure–activity relationship (SAR) studies pertaining to renal clearance on the series of pegylated pyrazine conjugates (Fig. 2).[26] These conjugates may be divided into two general categories. Compounds **4a–d** bear primary amino groups and absorb radiation in the blue region of the electromagnetic spectrum. Compounds **5–7** are all N-alkylated pyrazines and absorb radiation in the green region of the spectrum.

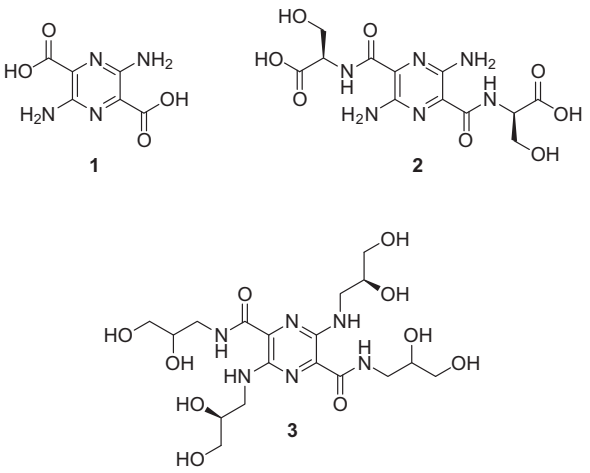

Figure 1. Pyrazine scaffold and its previously reported hydrophilic conjugates.

2. Results and discussion

2.1. Chemistry

During the synthesis of the low molecular weight hydrophilic conjugates of the type **2** and **3**, EDC–HOBt was employed in the initial coupling of pyrazinedicarboxylic acid **1** with protected amines in DMF to give the corresponding carboxamides in excellent yields (>70%).[21] However, such a coupling reaction with m-dPEG$_{12}$-amine **8c**[27] afforded only 35% yield of the desired **4c** on small scale after purification by reverse-phase preparative HPLC. Consequently, the reaction was carried out in the presence of several other coupling reagents like HBTU, HATU, BOP, and PyBOP to give 54%, 53%, 68%, and 75%, respectively of the m-dPEG derivative **4c**. Thus, PyBOP seems to be the reagent of choice and m-dPEG derivatives **4a**, **4b**, and **4d** were accessed in moderate to good yields by reacting **1** with m-dPEG-amines **8a**, **8b**, and **8d** respectively (Scheme 1).

The N-alkylated pyrazine derivatives **5a–c** were synthesized by reductive alkylation[28] of **4c** with the corresponding m-dPEG-aldehyde **9a–c** in the presence of 3 equiv each of HOAc and Na(OAc)$_3$BH in 1,2-dichloroethane (DCE), and the products were purified by reverse-phase preparative HPLC. Similarly, N-alkylated derivatives **6a**, **6b**, and **7a–c** were prepared by reductive alkylation of **4d** with propionaldehyde (**10a**), m-dPEG$_3$-aldehyde **10b**,[29] and m-dPEG-aldehydes **9b–d** respectively. It was found that additional amounts of reagents including aldehdyes were typically required to complete the reaction with lower molecular weight PEG–aldehydes ($m \leqslant 7$). It should be mentioned that the pyrazinecarboxamides **4c** and **4d** used in the synthesis of the corresponding N-alkylated analogs were not always purified by reverse-phase preparative HPLC. The crude products were either filtered through YMC C18 silica gel or dialyzed quickly using SpectraPor 7 dialysis tubing (MWCO 1000) to remove the excess reagents and the semi-pure compounds were used as such in subsequent reactions most of the time.

2.2. In vitro studies

The absorption (λ_{abs}) and emission (λ_{em}) maxima and plasma protein binding (PPB) were measured for the PEG–pyrazine conjugates **4a–d**, **5a–c**, **6a–b**, and **7a–c**. The results are summarized in Table 1, along with previously reported data for the small molecule pyrazines **2** and **3** and GFR standard iothalamate. The PEG–pyrazine derivatives bearing primary amino groups **4a–d** exhibited absorption maxima in the range of 435–440 nm (blue) and emission maxima in the range of 555–560 nm (green). The N-alkylated PEG–pyrazines **5a–c**, **6a–b** and **7a–c** exhibited absorption maxima in the range of 490–500 nm (green) and emission maxima in the range of 595–610 nm (orange).

Protein binding results indicated that the diaminopyrazines **4a–d** bind minimally to plasma proteins with PPB <5%, which are similar to or better than that of currently accepted GFR standard iothalamate. Compounds **5a–c**, obtained by N-alkylation of **4c**, exhibited negligible protein binding analogous to the parent compound. On the other hand, N-alkylation of **4d** resulted in analogs **6** and **7** that displayed varying levels of protein binding depending on the size of the groups. As would be expected, compound **6a** that contain hydrophobic propyl groups, showed 13% protein binding. In the PEG series **6b** and **7a–c**, protein binding increased with increasing PEG size, and compounds **7b** and **7c** exhibited as much as 40% protein binding.

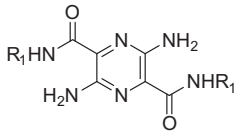

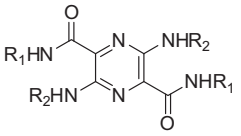

4a: $R_1 = (CH_2CH_2O)_4CH_3$

4b: $R_1 = (CH_2CH_2O)_8CH_3$

4c: $R_1 = (CH_2CH_2O)_{12}CH_3$

4d: $R_1 = (CH_2CH_2O)_{24}CH_3$

5a: $R_1 = (CH_2CH_2O)_{12}CH_3$, $R_2 = CH_2(CH_2CH_2O)_4CH_3$

5b: $R_1 = (CH_2CH_2O)_{12}CH_3$, $R_2 = CH_2(CH_2CH_2O)_8CH_3$

5c: $R_1 = (CH_2CH_2O)_{12}CH_3$, $R_2 = CH_2(CH_2CH_2O)_{12}CH_3$

6a: $R_1 = (CH_2CH_2O)_{24}CH_3$, $R_2 = CH_2CH_2CH_3$

6b: $R_1 = (CH_2CH_2O)_{24}CH_3$, $R_2 = (CH_2CH_2O)_3CH_3$

7a: $R_1 = (CH_2CH_2O)_{24}CH_3$, $R_2 = CH_2(CH_2CH_2O)_8CH_3$

7b: $R_1 = (CH_2CH_2O)_{24}CH_3$, $R_2 = CH_2(CH_2CH_2O)_{12}CH_3$

7c: $R_1 = (CH_2CH_2O)_{24}CH_3$, $R_2 = CH_2(CH_2CH_2O)_{24}CH_3$

Figure 2. Pegylated pyrazine-based GFR tracer agents.

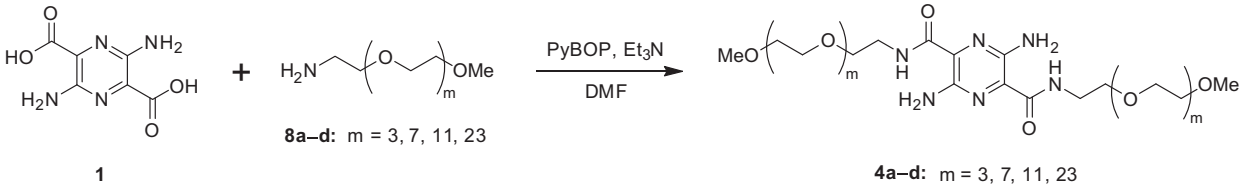

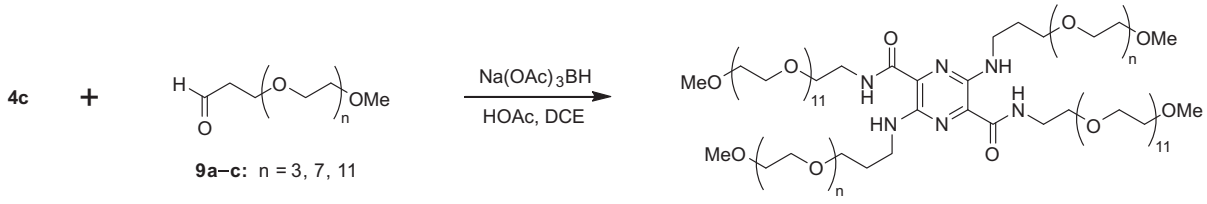

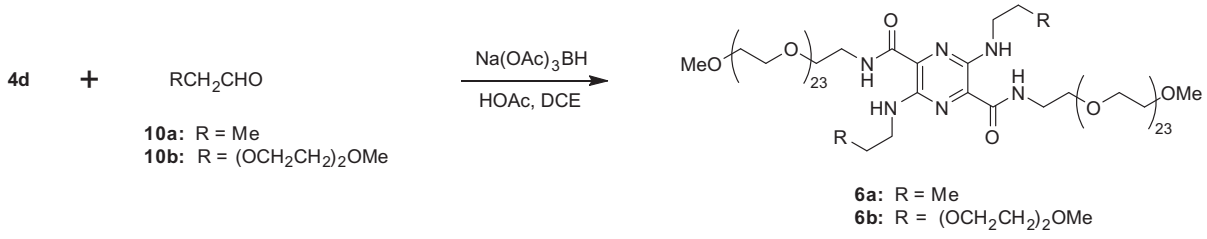

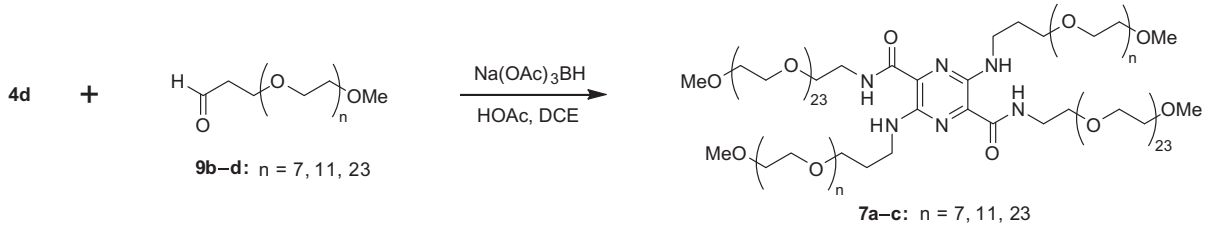

Scheme 1. Synthesis of hydrophilic PEG–pyrazine conjugates.

Table 1
Absorption, emission, plasma protein binding, and %ID recovery in urine

Compound	λ_{abs} (nm)	λ_{em} (nm)	PPB[a] (%)	%ID recovered in urine through 6 h[b]
Iothalamate	NA[c]	NA	10[d]	80 ± 2 (6)[e]
2	435	557	0	90 ± 1 (3)
3	484	594	6	88 ± 2 (3)
4a	436	557	0	41 ± 1 (6)
4b	438	557	0	45 ± 3 (6)
4c	437	558	0	71 ± 9 (3)
4d	439	559	5	96 ± 1 (6)
5a	491	603	0	86 ± 1 (3)
5b	498	605	1	87 ± 1 (3)
5c	499	604	3	97 ± 1 (3)
6a	496	611	13	85 ± 2 (3)
6b	490	594	11	96 ± 1 (3)
7a	498	602	30	92 ± 4 (3)
7b	499	602	41	89 ± 2 (3)
7c	495	603	39	86 ± 7 (3)

[a] Measured to ±3%.
[b] Results are expressed as the mean ± SEM.
[c] Not applicable.
[d] Reference[30].
[e] Numbers in parentheses indicate number of test animals.

2.3. In vivo studies

All in vivo studies were performed with Sprague–Dawley rats. All new compounds were profiled for urinary elimination and the urine was collected through 6 h after the administration of the tracer agent. Percent injected dose (%ID) of each compound recovered in the urine is given in Table 1. Among the PEG–pyrazine conjugates with diamino groups **4a**–**d**, increase in %ID recovered in urine was observed with concomitant increase in the length, molecular weight, and hydrodynamic volume of PEG side chains. This ultimately resulted in compound **4d** with two 24-mer PEGs displaying 96%ID recovered in urine after 6 h. Similarly, among the series **5a**–**c** obtained from **4c**, %ID recovered in the urine increased with increasing PEG size, and the compound **5c** with four 12-mer PEGs showed the highest %ID recovered in urine at 97%. In contrast, such a trend was not observed among the compounds in the series **6b** and **7a–c**. Compound **7c**, which contains four 24-mer PEGs displayed 86% recovery suggesting that there is a limit to the size of the PEG groups tolerated, and reaches an optimum value of 48 PEG units (cf. compounds **4d** and **5c**). Nevertheless, the %ID recovered in urine in all these compounds is superior (i.e. greater) to that of iothalamate. Compounds **7a–c** displayed elevated PPB values with respect to the other compounds that have high values of %ID recovered in urine. Since PEG polymers are highly hydrated with two water molecules per ethylene glycol unit,[31] it is possible that these compounds with relatively larger apparent molecular size are not readily filtered through the membrane in the ultrafiltration during the assay leading to higher measured protein binding compared to **4d**.

The pharmacokinetic profiles of PEG–pyrazine conjugates were assessed by determining plasma concentrations of the tracer agents by HPLC at 0, 2, 6, and 24 h post administration of the injected dose. A typical pharmacokinetic profile depicting plasma concentration of compound **5c** over time is shown in the Figure 3. Terminal phase plasma half-lives (related to k^{-1}) and steady state volume of distribution for selected compounds **4c**, **4d**, **5c**, and **7b**, along with comparators iothalamate and the small molecule pyrazine **2**, are given in Table 2. A trend toward shorter terminal half-life and lower volume of distribution with respect to both comparators is seen, which supports our strategy that PEGylation does minimize partitioning into the extracellular fluid producing a lower V_d and hence higher rate constant k, that could potentially lead to a faster GFR measurement. Compound **7b** containing more

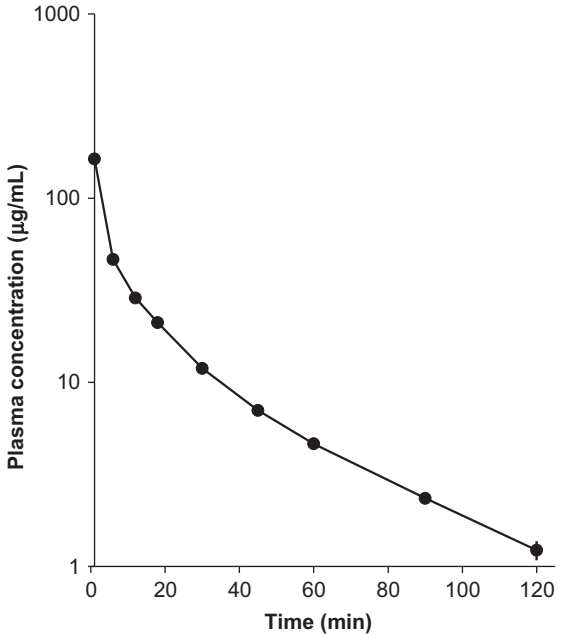

Figure 3. Plasma concentration versus time after bolus intravenous injection of **5c** in rat model.

Table 2
Plasma clearance half-lives, and steady-state volume of distribution for selected compounds[a,b]

Compound	Plasma half-life (min)	Plasma V_d (mL)
Iothalamate	32 ± 2 (4)[c]	104 ± 1
2	29 ± 1 (9)	83 ± 3
4c	20 ± 1 (3)	70 ± 2
4d	25 ± 1 (5)	64 ± 3
5c	19 ± 1 (3)	61 ± 1
7b	31 ± 3 (3)	68 ± 7

[a] Results are expressed as the mean ± SEM.
[b] Terminal phase half-life and volume of distribution from two compartment modeling.
[c] Numbers in parentheses indicate number of test animals.

Table 3
Effect of probenecid on the clearance of selected compounds[a]

Compound	Clearance (mL/min)	
	No probenecid	Probenecid (70 mg/kg)
^{99m}Tc-MAG$_3$	9.3 ± 0.4 (4)[b]	3.9 ± 0.6 (5)
Iothalamate	2.5 ± 0.2 (4)	2.2 ± 0.2 (5)
4d	2.8 ± 0.1 (5)	2.7 ± 0.2 (6)
5c	3.1 ± 0.2 (3)	3.3 ± 0.1 (3)

[a] The values are given as mean ± SEM.
[b] Numbers in parentheses indicate number of test animals.

than 48 PEG units cleared slower than all other pegylated derivatives. The optimal molecular size may have been reached with 48 PEG units (cf. compounds **4d** and **5c**), and it is possible that the diffusion of the relatively larger **7b** molecule out of the renal capillaries and into the glomerulus may be impeded due to its size. On the basis of SAR studies discussed so far, it can be concluded that the renal clearance properties of pegylated pyrazines **4d** and **5c** are clearly superior to that of the standard iothalamate.

To determine whether renal tubular secretion had any effect on the clearance of these pegylated compounds, separate pharmacokinetic experiments involving blockage of tubular secretion pathway using probenecid [*p*-(dipropylsulfamoyl)benzoic acid] were conducted.[32] The in vivo clearance of two selected pegylated pyrazine compounds **4d** and **5c** along with comparator iothalamate was measured with and without probenecid. In addition, ^{99m}Tc-MAG$_3$, a radioscintigraphic imaging agent that is known to clear via the tubular secretion pathway,[32,33] was employed as a positive control. The results of the blocking study are summarized in Table 3. While probenecid significantly decreased the clearance of ^{99m}Tc-MAG$_3$ ($p = 0.001$), it did not affect clearance of iothalamate ($p > 0.05$) as would be expected for non-GFR and GFR agents respectively. Similar to iothalamate, compounds **4d** and **5c** did not exhibit significant differences in clearance rates ($p > 0.05$) in the absence and presence of probenecid. Therefore, it can be concluded that compounds **4d** and **5c** are cleared exclusively by glomerular filtration in the rat model.

The noninvasive real-time monitoring of plasma clearance of the tracer agents was accomplished by optical methods in the rat model.[14] The time dependence of fluorescence measured at the rat ear post tail-vein injection of 1 mL of a 2 mM solution of the compound **5c** in PBS is shown in Figure 4. The clearance curve indicate a biphasic elimination profile with free distribution from blood into the tissue and the resultant fit of the data to a two compartment pharmacokinetic model gave a terminal half-life of about 22 min, which is comparable to plasma half-life of 19 min measured by invasive pharmacokinetic studies. Finally, in order to ascertain whether the optical clearance profile parallels actual concentration of the tracer in plasma, fluorescence response from the optical monitoring experiment was plotted against plasma concentration of **5c** obtained by HPLC analysis of the blood samples drawn at various intervals over the same time period (Fig. 5). As expected, optical measurement for clearance is very well correlated with the actual plasma concentration ($r^2 = 0.998$) in the terminal phase. Thus, plasma clearance of the tracer determined from fluorescence decay data can be reliably be used to estimate GFR.

3. Conclusions

Based on the fluorescence properties, plasma protein binding data, injected dose recovered in urine, probenecid blocking studies, plasma clearance data, and strong correlation between plasma concentration of the tracer and fluorescence intensity, the pegylated pyrazine compounds **4d** and **5c** are viable candidates for the measurement of GFR. In the rat animal model, these compounds displayed superior properties compared to iothalamate, which is currently an accepted standard for the measurement of GFR. These pegylated pyrazine compounds had a lower volume of distribution, lower terminal half-life, and a higher recovery in urine than previously reported small molecule pyrazine **2**.[21] Thus, a faster GFR measurement may be achieved with pegylated pyrazine than with the small molecule pyrazine. The noninvasive real-time monitoring of this class of compounds was demonstrated by following the clearance of **5c** by decrease in the fluorescence intensity measured at the ear as a function of time in the rat model. The selection of the clinical candidates based on secondary considerations such as cost, synthetic ease, toxicity, tissue optic properties, along with instrumental design and appropriate algorithms for accurate determination of GFR are in progress.

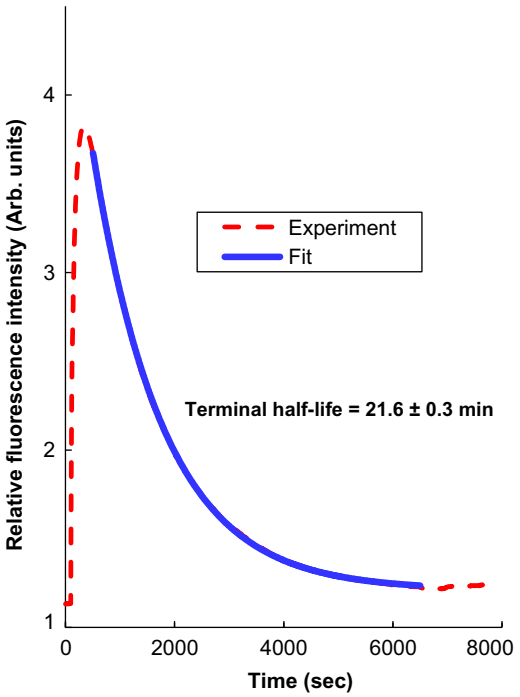

Figure 4. Fluorescence measured at the rat ear as a function of time for compound **5c**.

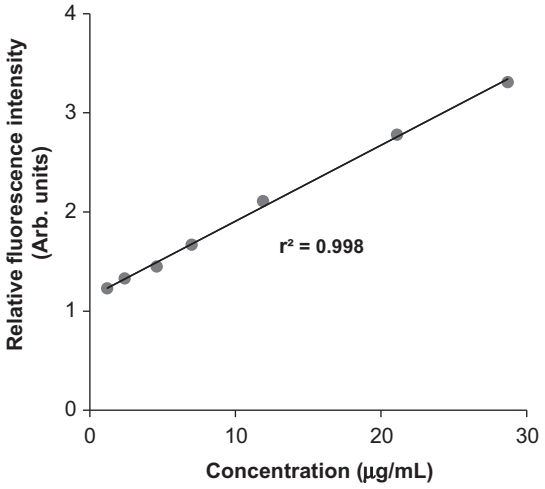

Figure 5. Correlation between plasma concentration and fluorescence intensity of **5c**.

4. Experimental

4.1. Chemistry

Unless otherwise noted, all solvents and reagents were used as supplied. Organic extracts were dried over either anhyd Na_2SO_4 or anhyd $MgSO_4$ and filtered using a fluted filter paper (P8) or a fritted glass funnel. Solvents were removed on a rotary evaporator under reduced pressure. RP-LC/MS (ESI, positive ion mode) analyses were carried out on either a BDS Hypersil C18 3 μm (50 × 4.6 mm) or a ThermoElectron Hypersil Gold C18 3 μm (50 × 4.6 mm) column. Compounds were injected using a gradient condition (5% B/0 min, 5% B/1 min, 95% B/4 min, 95% B/6 min) with a flow rate of 1 mL/min (mobile phase A: 0.05% TFA in H_2O; mobile phase B: 0.05% TFA in CH_3CN; λ_{max}: PDA (200–600 nm). Preparative RP-HPLC was carried out using a Waters XBrdige™ Prep C18 5 μm OBD™ 30 × 150 mm [λ_{max}: PDA (200–800 nm); flow: 50 mL/min; gradient: 5 to 30–40 to 95% B/7–25 min; mobile phase A: 0.1% TFA in H_2O; mobile phase B: 0.1% TFA in CH_3CN]. Certain compounds required the removal of TFA prior to additional in vivo studies. In these cases, free amines were isolated by washing with $NaHCO_3$. RP-HPLC analyses were carried out using a Phenomenex Luna 5 μm C18(2) 100 Å 250 × 4.6 mm column [λ_{max}: 264 or 280 nm; flow: 1 mL/min; gradient: 20% B/0 min, 20% B/3 min, 80% B/20 min; mobile phase A: 0.1% TFA in H_2O; mobile phase B: 0.1% TFA in CH_3CN)], and the chromatographic purities of all the compounds were ⩾95%. UV/Vis and Fluorescence spectra were measured on a Shimadzu UV-3101 PC and Jobin Yvon Fluorolog®-3 spectrometers respectively. NMR spectra were recorded on either a Varian Gemini-300 or a VNMRS-500 spectrometer. ^1H Chemical shifts are expressed in parts per million (δ) relative to TMS ($\delta = 0$) as an internal standard. ^{13}C Chemical shifts are referenced to either TMS ($\delta = 0$) or the residual solvent peaks in the spectra. Coupling constants (J) are reported in Hz. HRMS (ESI) data was obtained on a ThermoFisher LTQ-Orbitrap mass spectrometer equipped with an IonMax electrospray ionization source in FTMS mode with resolution ⩾30 K. Elemental analyses were carried out by Atlantic Microlab, Inc., Norcross, GA.

4.1.1. Representative procedure for the preparation of pyrazine carboxmide 4c and its analogs 4a, 4b, and 4d. 3,6-Diamino-*N*^{2},*N*^{5}-di(2,5,8,11,14,17,20,23,26,29,32,35-dodecaoxaheptatriacontan-37-yl)pyrazine-2,5-dicarboxamide (4c)

A 2 litre round-bottom flask equipped with a magnetic stir bar was charged with diacid **1** (3.50 g, 17.7 mmol),[34,35] m-dPEG12-amine (**8c**, 22.5 g, 40.2 mmol), and PyBOP (21.4 g, 41.1 mmol) in anhyd DMF (1 L) and purged with argon. Then Et_3N (50 mL) was slowly added to the suspension, and within an hour, all the reactants appeared dissolved leading to a dark red solution. The reaction mixture was stirred overnight at rt, concentrated under high vacuum to give 30.8 g of the crude product as dark red oil, which was subjected to purification by reverse phase preparative HPLC [column: Waters XBrdige™ Prep C18 5 μm OBD™ 30 × 150 mm; λ_{max}: PDA (200–800 nm), flow rate: 50 mL/min; gradient: mobile phase A:B 95:5/0 min, 95:5/1 min, 50:50/8 min, 5:95/8.1 min, 5:95/10 min (A: 0.1% TFA/H_2O, B: 0.1% TFA/CH_3CN)]. The product containing fractions were concentrated in vacuo, the residue was dissolved in $CHCl_3$ (150 mL), and washed successively with satd. $NaHCO_3$ (2 × 75 mL) and brine (75 mL). The $CHCl_3$ layer was dried over Na_2SO_4, filtered, and evaporated to dryness. The gummy residue was co-evaporated with 200 proof EtOH and then dried overnight under high vacuum at 40 °C to give **4c** (13.4 g, 59%) as bright orange solid: ^1H NMR ($CDCl_3$) δ 8.13 (t, J = 5.8 Hz, 2H), 6.06 (s, 4H), 3.69–3.54 (m, 96H), 3.38 (s, 6H); ^{13}C NMR ($CDCl_3$) δ 165.3, 146.6, 126.9, 71.9, 70.6, 70.59, 70.56, 70.5, 70.4, 69.8, 59.0, 39.0; RP-LC/MS (ESI) m/z 1281.9 $(M+H)^+$ (t_R = 3.76 min). Anal. Calcd for $C_{56}H_{108}N_6O_{26}$: C, 52.49; H, 8.49; N, 6.56. Found: C, 52.23; H, 8.44; N, 6.50.

4.1.1.1. 3,6-Diamino-*N*^{2},*N*^{5}-di(2,5,8,11-tetraoxatridecan-13-yl)pyrazine-2,5-dicarboxamide (4a). Orange gum, 0.99 g (65%, salt with TFA): ^1H NMR ($CDCl_3$) δ 8.16 (t, J = 5.7 Hz, 2H), 4.68 (br, 4H), 3.70–3.54 (m, 32H), 3.37 (s, 6H); ^{13}C NMR ($CDCl_3$) δ 165.3, 146.6, 127.0, 71.9, 70.62, 70.58, 70.55, 70.5, 70.4, 69.8, 59.0, 39.1; RP-LC/MS (ESI) m/z 577.5 $(M+H)^+$ (t_R = 3.78 min). HRMS (ESI) m/z calcd for $C_{24}H_{45}N_6O_{10}$ $(M+H)^+$ 577.3192, found 577.3193; calcd for $C_{24}H_{44}N_6O_{10}Na$ $(M+Na)^+$ 599.3011, found 599.3009.

4.1.1.2. 3,6-Diamino-*N*^{2},*N*^{5}-di(2,5,8,11,14,17,20,23-octaoxapentacosan-25-yl)pyrazine-2,5-dicarboxamide (4b). Orange gum, 0.99 g (78%, salt with TFA): ^1H NMR ($CDCl_3$) δ 8.16 (t, J = 5.8 Hz, 2H), 4.20 (br s, 4H), 3.69–3.54 (m, 64H), 3.38 (s, 6H); ^{13}C NMR ($CDCl_3$) δ 165.4, 159.7, 159.4, 71.9, 70.6, 70.47, 70.46, 70.4, 60.8, 59.0, 39.1; RP-LC/MS (ESI) m/z 930.1 $(M+H)^+$ (t_R = 3.88 min). HRMS (ESI) m/z calcd for $C_{40}H_{77}N_6O_{18}$ $(M+H)^+$ 929.5289, found 929.5303; calcd for $C_{40}H_{76}N_6O_{18}Na$ $(M+Na)^+$ 951.5108, found 951.5119.

4.1.1.3. 3,6-Diamino-*N*^{2},*N*^{5}-di(2,5,8,11,14,17,20,23,26,29,32,35,38,41,44,47,50,53,56,59,62,65,68,71-tetracosaoxatriheptacont an-73-yl)pyrazine-2,5-dicarboxamide (4d). Red solid, 20.0 g (61%): ^1H NMR ($CDCl_3$) δ 8.13 (t, J = 5.8 Hz, 2H), 6.06 (s, 4H), 3.68–3.54 (m, 192H), 3.38 (s, 6H); ^{13}C NMR ($CDCl_3$) δ 165.3, 146.6, 126.9, 71.9, 70.63, 70.6, 70.56, 70.5, 70.4, 69.8, 59.0, 39.0; RP-LC/MS (ESI) m/z 1179.1 $(M+H+NH_4)^{2+}$, 1182.0 $(M+H+Na)^{2+}$ (t_R = 3.88 min). Anal. Calcd for $C_{104}H_{204}N_6O_{50}$: C, 53.41; H, 8.79; N, 3.59. Found: C, 53.15; H, 8.81; N, 3.61.

4.1.2. Representative procedure for the preparation of N-alkylated pyrazine carboxmide 5c and its analogs 5a, 5b, 6a, 6b, and 7a–c. 3,6-Bis(2,5,8,11,14,17,20,23,26,29,32,35-dodecaoxaoctatriacontan-38-ylamino)-*N*^{2},*N*^{5}-di(2,5,8,11,14,17,20,23,26,29,32,35-dodecaoxaheptatriacontan-37-yl)pyrazine-2,5-dicarboxamide (5c)

A 500 mL round-bottom flask equipped with a magnetic stir bar was charged with bis-amide **4c** (6.24 g, 4.87 mmol) and dissolved in anhydrous 1,2-dichloroethane (DCE, 100 mL) under argon atmosphere. To the resulting orange solution, a solution of m-dPEG$_{12}$-propionaldehyde (7.34 g, 12.8 mmol) in DCE (25 mL) and glacial HOAc (0.73 mL, 12.7 mmol) were added in succession. Then sodium triacetoxyborohydride (2.71 g, 12.8 mmol) was introduced in 0.50 g portions over a 1.5 h period each time rinsing the transferring vial with additional DCE (75 mL total). The resulting reddish suspension was stirred overnight at rt in an atmosphere of argon and the reaction was quenched by a slow addition of saturated $NaHCO_3$ (100 mL). The biphasic mixture was stirred for 30 min, layers were separated, and the aqueous phase was further extracted with $CHCl_3$ (50 mL). The combined organic extracts were washed with brine (100 mL) and then dried over Na_2SO_4. Removal of solvents in vacuo gave 12.8 g the crude product as a red solid, which was subjected to purification by reverse phase preparative HPLC [column: Waters XBrdige™ Prep C18 5 μm OBD™ 50 × 250 mm; λ_{max}: 280 nm, flow rate: 50 mL/min; gradient: mobile phase A:B 75:25/0 min, 75:25/5 min, 45:55/40 min, 5:95/40.01 min, 5:95/45 min (A: 0.1% TFA/H_2O, B: 0.1% TFA/CH_3CN)]. The product containing fractions were concentrated in vacuo, the residue was dissolved in $CHCl_3$ (200 mL), and washed successively with satd. $NaHCO_3$ (2 × 100 mL) and brine (100 mL). The $CHCl_3$ layer was dried over Na_2SO_4, filtered, and evaporated to dryness. The red viscous residue was co-evaporated with 200 proof EtOH and then dried overnight under high vacuum at 40 °C to give **5c**

(7.40 g, 63%) as brick red solid: ^{1}H NMR (DMSO-d_6) δ 8.42 (t, J = 5.8 Hz, 2H), 7.88 (t, J = 5.5 Hz, 2H),3.64–3.34 (m, 192H), 3.23 (s, 12H), 1.79–1.75 (quintet, J = 6.4 Hz, 4H); ^{13}C NMR (DMSO-d_6) δ 165.9, 145.9, 126.3, 71.7, 70.28, 70.25, 70.2, 70.12, 70.09, 70.05, 69.3, 68.8, 58.5, 39.0, 38.1, 29.8; RP-LC/MS (ESI) m/z 2394.5 $(M+H)^+$, 1197.7 $(M+2H)^{2+}$ (t_R = 4.09 min). Anal. Calcd for $C_{108}H_{212}N_6O_{50}$: C, 54.16; H, 8.92; N, 3.51. Found: C, 54.31; H, 8.91; N, 3.52.

4.1.2.1. 3,6-Bis(2,5,8,11-tetraoxatetradecan-14-ylamino)-N^2,N^5-di(2,5,8,11,14,17,20,23,26,29,32,35-dodecaoxaheptatriacontan-37-yl)pyrazine-2,5-dicarboxamide (5a). Red oil, 0.391 g (28% for two steps, salt with TFA): ^{1}H NMR (DMSO-d_6) δ 8.42 (t, J = 6.0 Hz, 2H), 3.56–3.40 (m, 128H), 3.24, 3.22 (2 × s, 12H), 1.80–1.75 (quintet, J = 6.4 Hz, 4H); ^{13}C NMR (DMSO-d_6) δ 165.9, 145.9, 126.3, 71.74, 71.73, 70.29, 70.28, 70.24. 70.2, 70.12, 70.1, 70.0, 69.3, 68.8, 58.49, 58.48, 39.0, 38.1, 29.7; RP-LC/MS (ESI) m/z 854.1 $(M+H+NH_4)^{2+}$ (t_R = 4.11 min). HRMS (ESI) m/z calcd for $C_{76}H_{149}N_6O_{34}$ $(M+H)^+$ 1690.0109, found 1690.0182; calcd for $C_{76}H_{148}N_6O_{34}Na$ $(M+Na)^+$ 1711.9929, found 1711.9989.

4.1.2.2. 3,6-Bis(2,5,8,11,14,17,20,23-octaoxahexacosan-26-ylamino)-N^2,N^5-di(2,5,8,11,14,17,20,23,26,29,32,35-dodecaoxaheptatriacontan-37-yl)pyrazine-2,5-dicarboxamide (5b). Red oil, 0.237 g (14% for two steps, salt with TFA): ^{1}H NMR (DMSO-d_6) δ 8.41 (t, J = 6.0 Hz, 2H), 3.56–3.40 (m, 160H), 3.24, 3.22 (2 × s, 12H), 1.79–1.74 (quintet, J = 6.4 Hz, 4H); ^{13}C NMR (DMSO-d_6) δ 165.9, 145.9, 126.3, 71.7, 70.28, 70.24, 70.2, 70.12, 70.09, 70.05, 69.3, 68.8, 58.5, 39.0, 38.1, 29.8; RP-LC/MS (ESI) m/z 1022.2 $(M+2H)^{2+}$ (t_R = 4.11 min). HRMS (ESI) m/z calcd for $C_{92}H_{181}N_6O_{42}$ $(M+H)^+$ 2042.2206, found 2042.2082; calcd for $C_{92}H_{180}N_6O_{42}Na$ $(M+Na)^+$ 2064.2026, found 2064.2030.

4.1.2.3. 3,6-Bis(propylamino)-N^2,N^5-di(2,5,8,11,14,17,20,23,26,29,32,35,38,41,44,47,50,53,56,59,62,65,68,71-tetracosaoxatriheptacontan-73-yl)pyrazine-2,5-dicarboxamide (6a). Brick red sticky solid, 0.281 g (13% for two steps, salt with TFA): ^{1}H NMR (DMSO-d_6) δ 8.40 (t, J = 6.0 Hz, 2H), 3.64–3.33 (m, 196H), 3.22 (s, 6H), 1.58–1.51 (sextet, J = 7.0 Hz, 4H), 0.92 (t, J = 7.4 Hz, 6H); RP-LC/MS (ESI) m/z 808.6 $(M+3H)^{3+}$ 1212.2 $(M+2H)^{2+}$ (t_R = 4.18 min). HRMS (ESI) m/z calcd for $C_{110}H_{218}N_6O_{56}$ $(M+2H)^{2+}$ 1211.7345, found 1211.7343; calcd for $C_{110}H_{217}N_6O_{56}Na$ $(M+H+Na)^{2+}$ 1222.7254, found 1222.7256.

4.1.2.4. 3,6-Bis((2-(2-(2-methoxyethoxy)ethoxy)ethyl)amino)-N^2,N^5-di(2,5,8,11,14,17,20,23,26,29,32,35,38,41,44,47,50,53,56,59,62,65,68,71-tetracosaoxatriheptacontan-73-yl)pyrazine-2,5-dicarboxamide (6b). Red gum, 0.538 g (39% for two steps, salt with TFA): ^{1}H NMR (DMSO-d_6) δ 8.50 (br t, 2H), 4.15 (br, 2H), 3.66–3.34 (m, 216H), 3.24, 3.23 (2 × s, 6H); RP-LC/MS (ESI) m/z 1315.73 $(M+2H)^{2+}$, 877.27 $(M+3H)^{3+}$ (t_R = 16.11 min), 1325.3 $(M+H+NH_4)^{2+}$ (t_R = 4.04 min). HRMS (ESI) m/z calcd for $C_{118}H_{233}N_6O_{56}Na$ $(M+H+Na)^{2+}$ 1326.7728, found 1326.7721; calcd for $C_{118}H_{232}N_6O_{56}Na$ $(M+Na)^+$ 2652.5383, found 2652.5328.

4.1.2.5. 3,6-Bis(2,5,8,11,14,17,20,23-octaoxahexacosan-26-ylamino)-N^2,N^5-di(2,5,8,11,14,17,20,23,26,29,32,35,38,41,44,47,50,53,56,59,62,65,68,71-tetracosaoxatriheptacontan-73-yl)pyrazine-2,5-dicarboxamide (7a). Brick red, 0.625 g (44% for two steps, salt with TFA): ^{1}H NMR (DMSO-d_6) δ 8.42 (t, J = 6.0 Hz, 2H), 7.90 (br, 2H), 3.67–3.40 (m, 256H), 3.24, 3.23 (2 × s, 12H), 1.80–1.75 (quintet, J = 6.4 Hz, 4H); RP-LC/MS (ESI) m/z 1033.7 $(M+3H)^{3+}$, 1559.3 $(M+H+NH_4)^{2+}$ (t_R = 4.08 min). HRMS (ESI) m/z calcd for $C_{140}H_{276}N_6O_{66}Na_2$ $(M+2Na)^{2+}$ 1571.9105, found 1571.9145.

4.1.2.6. 3,6-Bis(2,5,8,11,14,17,20,23,26,29,32,35-dodecaoxaoctatriacontan-38-ylamino)-N^2,N^5-di(2,5,8,11,14,17,20,23,26,29,32,35,38,41,44,47, 50,53,56,59,62, 65,68,71-tetracosaoxatriheptacontan-73-yl)pyrazine-2,5-dicarboxamide (7b). Red solid, 1.84 g (36% for two steps): ^{1}H NMR (DMSO-d_6) δ 8.41 (t, J = 5.9 Hz, 2H), 7.88 (t, J = 5.5 Hz, 2H), 3.55–3.41 (m, 288H), 3.233, 3.230 (2 × s, 12H), 1.79–1.74 (quintet, J = 6.4 Hz, 4H); ^{13}C NMR (DMSO-d_6) δ 165.9, 145.9, 126.3, 71.7, 70.28, 70.25, 70.2, 70.12, 70.1, 70.05, 58.5, 39.0, 38.1, 29.8. Anal. Calcd for $C_{156}H_{308}N_6O_{74}$: C, 54.28; H, 8.99; N, 2.43. Found: C, 54.09; H, 9.03; N, 2.41.

4.1.2.7. 3,6-Bis(2,5,8,11,14,17,20,23,26,29,32,35,38,41,44,47,50,53,56,59,62,65,68,71-tetracosaoxatetraheptacontan-74-ylamino)-N^2,N^5-di(2,5,8,11,14,17,20,23,26,29,32,35,38,41,44,47,50,53,56,59,62,65,68,71-tetracosaoxatriheptacontan-73-yl)pyrazine-2,5-dicarboxamide (7c). Brick red solid, 0.869 g (23% for two steps, salt with TFA): ^{1}H NMR (DMSO-d_6) δ 8.46 (t, J = 5.8 Hz, 2H), 7.95 (br, 2H), 3.63–3.42 (m, 384H), 3.24 (s, 12H), 1.80–1.75 (quintet, J = 6.4 Hz, 4H). HRMS (ESI) m/z calcd for $C_{204}H_{404}N_6O_{98}Na_4$ $(M+4Na)^{4+}$ 1149.6596, found 1149.6617.

4.2. In vitro characterization and In vivo studies

In general, each test compound was dissolved in phosphate buffered saline (PBS) to form a 2 mM stock solution and further diluted with PBS as needed.

4.2.1. Photophysical properties and protein binding

The UV absorbance properties were measured on a 100 μM solution and the fluorescence properties were determined on a 10 μM solution. The percent plasma protein binding was determined on a 20 μM compound solution in rat plasma incubated at 37 °C for 1 h, and the detailed procedures were described elsewhere.[21]

4.2.2. Injected dose recovery in urine, invasive pharmacokinetic, and probenecid inhibition studies

Recovery of the injected dose in urine studies were conducted in either conscious or anesthetized Sprague-Dawley rats. Invasive pharmacokinetic and probenecid studies were carried out in male Sprague-Dawley rats (330–380 g) that were anesthetized by Inactin (I.P.). In each of the experiments, 1 mL of 2 mM test compound was administered per rat. The detailed experimental procedures and the data analyses were described elsewhere.[21]

4.2.3. Noninvasive optical monitoring studies

Non-invasive optical monitoring studies were performed on male Sprague–Dawley rats that were anesthetized by Inactin (I.P.) or 2% isoflurane. The test compound (1 mL, 2 mM in PBS) was injected into the tail-vein of the rat and the fluorescence signal corresponding to plasma and tissue distribution and subsequent renal clearance of the compound was monitored at the ear by placing it near the common end of the bifurcated fiber optic bundle that was attached to a laser source (473 nm solid state) and a detector system. The pharmacokinetic parameters of the compounds were analyzed using WinNonLin pharmacokinetic modeling software (Pharsight, Mountain View, CA) and Microsoft (Redmond, Washington) Excel.

Acknowledgements

We thank Dr. Carlos Rabito of the Harvard University Medical School and Massachusetts General Hospital, Professor Thomas Dowling of the University of Maryland, Dr. Sevag Demirjian of the Cleveland Clinic Foundation, and Dr. Joseph Nally of the Cleveland Clinic Foundation for their insightful discussions and advice.

We thank our Covidien Pharmaceutical colleagues Jolette K. Wojdyla, Tim A. Marzan, Rana Kumar, Tasha M. Schoenstein, Dr. J. Micah Wilcox, Dr. James G. Kostelc, Dr. Bich T. Vu, and Dr. Jingyue Yang for their experimental and analytical support.

References and notes

1. Levey, A. S.; Coresh, J.; Balk, E.; Kausz, A. T.; Levin, A.; Steffes, M. W.; Hogg, R. J.; Perrone, R. D.; Lau, J.; Eknoyan, G. *Ann. Intern. Med.* **2003**, *139*, 137.
2. Rule, A. D.; Larson, T. S.; Bergstralh, E. J.; Slezak, J. M.; Jacobsen, S. J.; Cosio, F. G. *Ann. Intern. Med.* **2004**, *141*, 929.
3. Traynor, J.; Mactier, R.; Geddes, C. C.; Fox, J. G. *BMJ* **2006**, *333*, 733.
4. Stevens, L. A.; Levey, A. S. *Ann. Intern. Med.* **2004**, *141*, 959.
5. Stevens, L. A.; Coresh, J.; Greene, T.; Levey, A. S. N. *Engl. J. Med.* **2006**, *354*, 2473.
6. Verhave, J. C.; Fesler, P.; Ribstein, J.; du Cailar, G.; Mimran, A. *Am. J. Kidney Dis.* **2005**, *46*, 233.
7. Diskin, C. J. *Nephrol. Dial. Transplant.* **2006**, *21*, 3338.
8. Prigent, A. *Semin. Nucl. Med.* **2008**, *38*, 32.
9. Stevens, L. A.; Levey, A. S. *J. Am. Soc. Nephrol.* **2009**, *20*, 2305.
10. Dowling, T. C.; Frye, R. F.; Fraley, D. S.; Matzke, G. R. *Pharmacotherapy* **1999**, *19*, 943.
11. Agarwal, R. *Am. J. Kidney Dis.* **2003**, *41*, 752.
12. Rabito, C. A.; Moore, R. H.; Bougas, C.; Dragotakes, S. C. *J. Nucl. Med.* **1993**, *34*, 199.
13. Rabito, C. A.; Panico, F.; Rubin, R.; Tolkoff-Rubin, N.; Teplick, R. *J. Am. Soc. Nephrol.* **1994**, *4*, 1421.
14. Dorshow, R. B.; Bugaj, J. E.; Burleigh, B. D.; Duncan, J. R.; Johnson, M. A.; Jones, W. B. *J. Biomed. Opt.* **1998**, *3*, 340.
15. Yu, W.; Sandoval, R. M.; Molitoris, B. A. *Am. J. Physiol. Renal Physiol.* **2007**, *292*, F1873.
16. Schock-Kusch, D.; Sadick, M.; Henninger, N.; Kraenzlin, B.; Claus, G.; Kloetzer, H.-M.; Weib, C.; Pill, J.; Gretz, N. *Nephrol. Dial. Transplant.* **2009**, *24*, 2997.
17. Wang, E.; Sandoval, R. M.; Campos, S. B.; Molitoris, B. A. *Am. J. Renal Physiol.* **2010**, *299*, F1048.
18. Schock-Kusch, D.; Xie, Q.; Shulhevich, Y.; Hesser, J.; Stsepankou, D.; Sadick, M.; Koenig, S.; Hoecklin, F.; Pill, J.; Gretz, N. *Kidney Int.* **2011**, *79*, 1254.
19. Rabito, C. A.; Chen, Y.; Schomacker, K. T.; Modell, M. D. *Appl. Opt.* **2005**, *44*, 5956.
20. Chinen, L.; Galen, K. P.; Kuan, K. T.; Dyszlewski, M. E.; Ozaki, H.; Sawai, H.; Pandurangi, R. S.; Jacobs, F. G.; Dorshow, R. B.; Rajagopalan, R. *J. Med. Chem.* **2008**, *51*, 957.
21. Rajagopalan, R.; Neumann, W. L.; Poreddy, A. R.; Fitch, R. M.; Freskos, J. N.; Asmelash, B.; Gaston, K. R.; Galen, K. P.; Shieh, J.-J.; Dorshow, R. B. *J. Med. Chem.* **2011**, *54*, 5048.
22. Hedaya, M. A. *Basic Pharmacokinetics*; CRC Press: Boca Raton, FL, 2007.
23. Harris, J. M.; Martin, N. E.; Modi, M. *Clin. Pharmacokinet.* **2001**, *40*, 539.
24. Hamidi, M.; Azadi, A.; Rafiei, P. *Drug Delivery* **2006**, *13*, 399.
25. Yamaoka, T.; Tabata, Y.; Ikada, Y. *J. Pharm. Sci.* **1994**, *83*, 601.
26. Presented in part: Poreddy, A. R.; Asmelash, B.; Debreczeny, M. P.; Fitch, R. M.; Freskos, J. N.; Galen, K. P.; Gaston, K. R.; Kostelc, J. G.; Kumar, R.; Marzan, T. A.; Neumann, W. L.; Rajagopalan, R.; Schoenstein, T. M.; Shieh, J.-J.; Wilcox, J. M.; Wojdyla, J. K.; Dorshow, R. B. In *Reporters, Markers, Dyes, Nanoparticles, and Molecular Probes for Biomedical Applications III*; Achilefu, S., Raghavachari, R., Eds.; SPIE Press: Bellingham, WA, 2011; Vol. 7910,.
27. All the monomethoxy(polyethylene glycol) (m-dPEG) reagents used are discrete, i.e., monodisperse and were purchased from Quanta BioDesign, Ltd, Powell, Ohio.
28. Poreddy, A. R.; Asmelash, B.; Neumann, W. L.; Dorshow, R. B. *Synthesis* **2010**, 2383.
29. Carlise, J. R.; Kriegel, R. M.; Reese, W. S., Jr.; Weck, M. *J. Org. Chem.* **2005**, *70*, 5550.
30. Prueksaritanont, T.; Lui, C. Y.; Lee, M. G.; Chiou, W. L. *Biopharm. Drug Dispos.* **1986**, *7*, 347.
31. Harris, J. M.; Chess, R. B. *Nat. Rev. Drug. Discov.* **2003**, *2*, 214.
32. Fritzberg, A. R.; Kasina, S.; Eshima, D.; Johnson, D. L. *J. Nucl. Med.* **1986**, *27*, 111.
33. Bubeck, B.; Brandau, W.; Weber, E.; Kälble, T.; Parekh, N.; Georgi, P. *J. Nucl. Med.* **1990**, *31*, 1285.
34. Taylor, E. C., Jr.; Loux, H. M.; Falco, E. A.; Hitchings, G. H. *J. Am. Chem. Soc.* **1955**, *77*, 2243.
35. Shirai, K.; Yanagisawa, A.; Takahashi, H.; Fukunishi, K.; Matsuoka, M. *Dyes and Pigments* **1998**, *39*, 49.